JOURNAL OF SOLID STATE CHEMISTRY 116, 157–169 (1995)

High Specific Surface Area Nickel Mixed Oxide Powders $LaNiO_3$ (Perovskite) and $NiCo_2O_4$ (Spinel) via Sol–Gel Type Routes for Oxygen Electrocatalysis in Alkaline Media

Mustapha El Baydi,* Shashi Kant Tiwari,*,† Ravindra Nath Singh,† Jean-Luc Rehspringer,‡ Pierre Chartier,*,[1] Jean François Koenig,* and Gérard Poillerat*

*Laboratoire d'Electrochimie et Chimie Physique du Corps Solide, URA au CNRS N°405, Faculté de Chimie, Université Louis Pasteur, 1–4 rue Blaise Pascal, 67000 Strasbourg, France; †Electrochemical Laboratory, Department of Chemistry, Faculty of Science, Banaras Hindu University, Varanasi 221005, India; and ‡Groupe des Materiaux Inorganiques, UMR 456 du CNRS, IPCMS, EHICS, 1 rue Blaise Pascal, 67000 Strasbourg, France

Received May 20, 1994; in revised form September 22, 1994; accepted September 23, 1994

A novel sol–gel process of preparation of oxide electrocatalysts is investigated to prepare Ni-containing mixed oxides $LaNiO_3$ and $NiCo_2O_4$ at moderate temperatures. High surface area (20–55 $m^2 g^{-1}$) powders and high roughness electrodes (30–1500) were obtained. Apparent and real electrocatalytical activity are compared and discussed. © 1995 Academic Press, Inc.

INTRODUCTION

Spinel-type mixed oxides AB_2O_4, in which A and B are transition metals, and perovskite-type mixed oxides ABO_3, in which A is a rare earth and B is a transition metal, are very often conductive materials and efficient electrocatalysts in electrosynthesis. Extensive reviews on conductive metal oxide electrodes by Trasatti (1) and on reactions at metal oxide electrodes by O'Sullivan and Calvo (2) include these two oxide families. More recently, the structure and reactivity of perovskite-type oxides in catalysis and electrocatalysis were reviewed by Tejuca *et al.* (3). Among all mixed oxides, Ni-containing oxides are very frequently the highest efficient. We have synthesized and investigated thin films of pure $NiCo_2O_4$ (4–9) and $LaNiO_3$ (10) deposited on conductive substrates either by spraying (reactive nebulization) or sequential coating, with the objective of investigating their electrocatalytical properties related to the oxygen reactions.

Although the efficiency of a catalyst is governed by the intrinsic activity of its surface active sites, one studies, in practice, catalytic and electrocatalytic materials having in addition high specific surfaces, i.e., specific surfaces higher than ca. 20 $m^2 g^{-1}$, in order to increase the quantity of the active surface sites per unit mass (catalysis) or per unit geometric area of a coated electrode (electrocatalysis). The sol–gel type processes for the synthesis of solids provide means of preparation of such high specific area materials, because they yield finely dispersed powders at temperatures usually lower than the other methods.

In electrocatalysis, oxides or mixed oxides of the transition metals are considered as electrode materials for such practical electrode reactions as oxygen or chlorine evolution, oxygen reduction, methanol oxidation, etc., but the sol–gel methods of preparation have received little attention, in contrast to direct ceramic sintering of the parent oxides, dry evaporation, freeze-drying, spraying, calcination of the coprecipitated metal hydroxides, or thermal decomposition of appropriate metal salts.

By sol–gel type preparation processes, one means in this paper not only the pristine sol–gel process, which is the obtention of materials from metal alkoxydes in organic media, but also the obtention of materials from inorganic or organo-inorganic precursors in organic or aqueous media. In each case, gel-like phases form out of solutions, but these amorphous and vitreous phases differ in structure with each method. The latter type of process, using hydroxy-acids (principally the citric acid) in aqueous medium, was originally employed for preparing perovskites of the type $LnMO_3$ (Ln = Y, La, Sm; M = V, Cr, Mn, Fe, Co, Ni) (11, 12). In contrast, sol–gel type processes have been only occasionally employed for preparing spinel-type oxides (13), but, to our knowledge, not for electrocatalysis.

Recently, we have reported on the preparation of the cobaltite of cobalt, Co_3O_4, which is a spinel, via a novel sol–gel process (14). This novel process involves the formation at 140°C of a vitreous gel of cobalt propionate $Co(CH_3CH_2CO_2)_2$, by dissolution of $CoCO_3$ in pure liquid

[1] To whom correspondence should be addressed.

0022-4596/95 $6.00

propionic acid CH_3CH_2COOH (i.e., $C_3H_6O_2$). The oxide Co_3O_4 was obtained, in a powder form, with a BET (Brunauer Emmett Teller) surface area as high as 28 $m^2\ g^{-1}$, after calcination in air at 300°C. This good result prompted us to investigate the syntheses of other mixed oxides via the above mentioned propionic acid process and, for the sake of comparison, via other sol–gel processes.

In this work, we extend our investigations to the two title nickel-containing mixed oxides: $NiCo_2O_4$ and $LaNiO_3$. $NiCo_2O_4$ is of spinel type, and $LaNiO_3$ is of perovskite type. The propionic acid sol–gel process used for Co_3O_4 (14) was adapted to both of them. The process clearly involves a pure organic liquid medium acting simultaneously as the reactant and as the solvent. It is compared to the conventional process which involves in water a reactive synergy between a hydroxy-acid and the nitrate ions (hydroxy-acid aided process) (15). For this comparison the malic acid, whose formula is $CH_2CHOH(COOH)_2$ (i.e., $C_4H_6O_5$), was selected as the hydroxy-acid. The report focuses on the syntheses, characterizations, specific surface areas and electrocatalytic activities of the new sol–gel $NiCo_2O_4$ and $LaNiO_3$ powders.

EXPERIMENTAL

Characterization Methods

The thermogravimetric + differential thermal analyses were performed with a TG–DTA Setaram 92 apparatus, under air flux and atmospheric pressure. Scanning electron microscopy photographs were obtained on a Jeol (JSM 840) SEM apparatus and X-ray diffractograms with a Guinier–Wolf chamber, using the $CoK\alpha_1$ radiation ($\lambda = 0.17889$ nm). The transmission infrared spectra were recorded by a Fourier transform Bruker spectrophotometer in KBr between 400 and 4000 cm^{-1}.

The BET specific surface areas, S_{BET}, of the powders were obtained using a Carlo Erba instrument (Sorpty 1750) using nitrogen gas.

The electrical conductivities of the $NiCo_2O_4$ powders were measured with a Keithley 227 ohmmeter on compressed bars, equipped with silver laque (Demetron) ohmic contacts. $LaNiO_3$ being quasi-metallic, the instrument was not sensitive enough, and no attempt was made to measure accurately its conductivity. Nevertheless the activation energies, E_a, of the conductivity with temperature for the two types of oxides were measured, under air, oxygen, and argon atmospheres, using a very thin layer of powder dry-brushed on quartz platelets, whose resistance was found measurable even with $LaNiO_3$ powders, and varying with the temperature. In that case, the ohmic contacts were made with a gold laque (Demetron). The resistances were measured with a Keithley ohmmeter 175A. Figure 1 shows a typical $\ln R$ vs $1/T$ curve, recorded with the powder of sol–gel $NiCo_2O_4$ synthesized from the propionic acid, after three or four heatings and coolings down. The other types of powders gave similar plots, showing always two linear segments.

Electrochemical Methods

The electroanalytical i–E curves (cyclic or stationary) were recorded using a Bruker ECP 133 potentiostat. Electrodes have been film electrodes, except for $LaNiO_3$ syn-

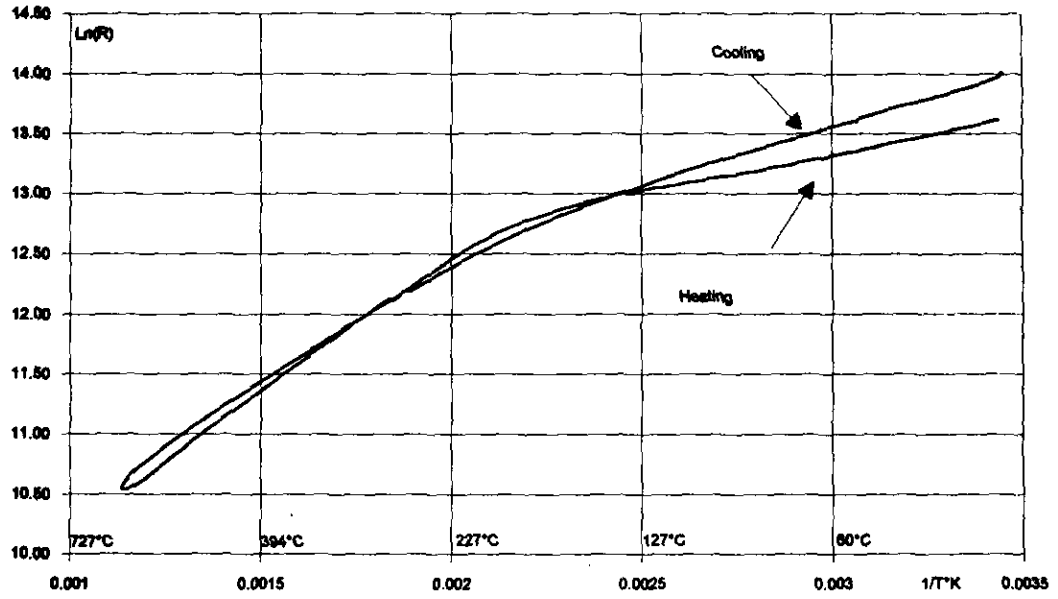

FIG. 1. Typical logarithmic variation of the resistance vs $1/T$ plot of a thin film of oxide spread on quartz by brushing. Oxide, $NiCo_2O_4$ (propionic acid); thickness, undetermined; atmosphere, air.

thesized from malic acid, in which case they were pellet electrodes. Film electrodes were made by painting a conductive substrate with a suspension of the powder in isopropylic alcohol, followed by a thermal treatment. The substrate were either 0.125-mm Ni foils (Aldrich, 99.9%) or graphited polyisobutylene, a conductive polymeric composite (Nikolaus Branz, Berlin). Pellet electrodes were prepared by first pressing the powder into 13-mm-diameter pellets at a pressure of 5 ton cm^{-2} and annealing at 600°C (100°C lower than the preparation temperature). The electrode was then made hydrophobic by dipping in 1% polystyrene solution in dichloromethane and drying at 100°C according to Calvo *et al.* (16). The process was repeated several times, and finally, the surface was polished with No. 1200 emery paper. The ohmic contacts were made using conductive silver paste (Demetron) and were carefully isolated from the solutions by Araldite epoxy glue (Ciba Geigy, Switzerland).

The roughness factors, ρ, of the test film electrodes were estimated from the intensities of the capacitive currents which were measured by cycling the potential with a scan rate $v = dE/dt$ in a narrow range (~±50 mV) in a double-layer region at the oxide/solution interface (i.e., in a region which is presumably exempt of pseudo-capacitive and faradaic currents). The roughness factor is defined as the ratio of the real surface area to the geometric area of a rugous film. Figure 2 shows such a typical cyclic voltammogram, pertaining to a film electrode made of sol–gel $NiCo_2O_4$ synthesized from propionic acid and painted on Ni. Similar voltammograms were obtained with all other electrodes. The capacity of reference, i.e., the capacity of an ideal oxide surface with a roughness factor unity was taken to be 60 $\mu F\ cm^{-2}$, following Levine and Smith (17). The roughness factor was therefore computed according to $\rho = C/60$, where C is the measured double layer capacity, i.e., the slope of the i vs v plots (taken at the middle potential of the scanning range).

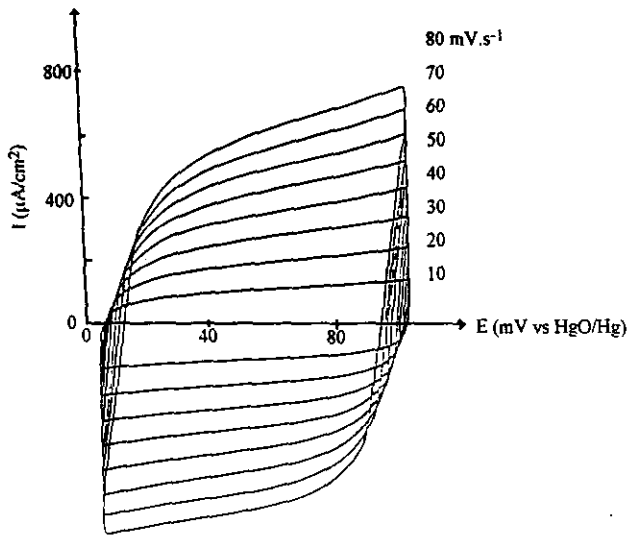

FIG. 2. Typical cyclic voltammograms of the interface of a sol–gel $NiCo_2O_4$ (propionic acid) film with 1 *M* KOH at $E = 0.05$ V vs HgO/Hg. Scanning range, ±50 mV; scanning rates, 10–80 mV sec^{-1}.

CHEMICAL SYNTHESES OF $NiCo_2O_4$ AND $LaNiO_3$

Chemicals

The syntheses of $NiCo_2O_4$ and $LaNiO_3$ were conducted using commercial grade reagents $Ni(NO_3)_2 \cdot 6H_2O$ (Merck, ref. 6743), $Co(NO_3)_2 \cdot 6H_2O$ (Merck, ref. 2536), $La(NO_3)_3 \cdot 6H_2O$ (Alfa, ref. 43121), Na_2CO_3 (Fluka, ref. 71345), propionic acid, (liquid, T_{eb} 141°C) C_2H_5COOH (Janssen Chimica, 14.930.89), and malic acid (solid, m.p. 100°C) $C_2H_3OH(COOH)_2$ (Lancaster, 3800). H_2O was distilled and then doubly permuted on resin (R-3, ref. 83002).

Synthesis of $NiCo_2O_4$ via the Propionic Acid Sol–Gel Type Route

The synthesis was started with a precipitated mixture of cobalt and nickel carbonates with the ratio Co : Ni equal to 2. The mixture was a coprecipitate which was obtained by addition of 1.5 *M* Na_2CO_3 to a 1 *M* $Co(NO_3)_2 \cdot 6H_2O$ + 0.5 *M* $Ni(NO_3)_2 \cdot 6H_2O$ aqueous solution (the synthesis could have been started with commercial carbonates either). The procedure follows as for Co_3O_4 (14): filtration and washings of the precipitate, dissolution in an excess of liquid CH_3CH_2COOH (150 ml per 100 g of mixed carbonate), and heating at 140°C, so that most of the excess water and propionic acid was evaporated, until the resinic gel was formed. The solution turned from opaque to limpid before to gel. The maroon gel hardened by cooling down to room temperature, and quick addition of liquid nitrogen powdered it.

No attempt was made to establish the detailed structure of the gel, which was characterized by IR transmission spectroscopy and thermogravimetric and differential thermal analysis (TGA–DTA, see below) only. The gel can be given the symbolic representation $NiCo_2(CO_3^{2-})_a(C_3H_5O_2^-)_b(C_3H_6O_2)_c$, in analogy with formulae proposed, for instance, by Anderton and Sale (18), to characterize such amorphous precursors. Such gels are known to contain, besides the forming ions, a quantity of neutral molecules and/or oligomers of the solvent and/or the reactant. The exact composition and structure determination would deserve crossed investigations, involving quantitative analyses of all the elements and of the evolved gases, and X-ray analysis in addition to thermogravimetry and IR spectroscopy, which only were used here. The powdered gel was then further heated at 180°C in an air flux for 1 to 2 hr, and, finally, was pyrolyzed in air at different temperatures (see below), yielding a black powder of $NiCo_2O_4$.

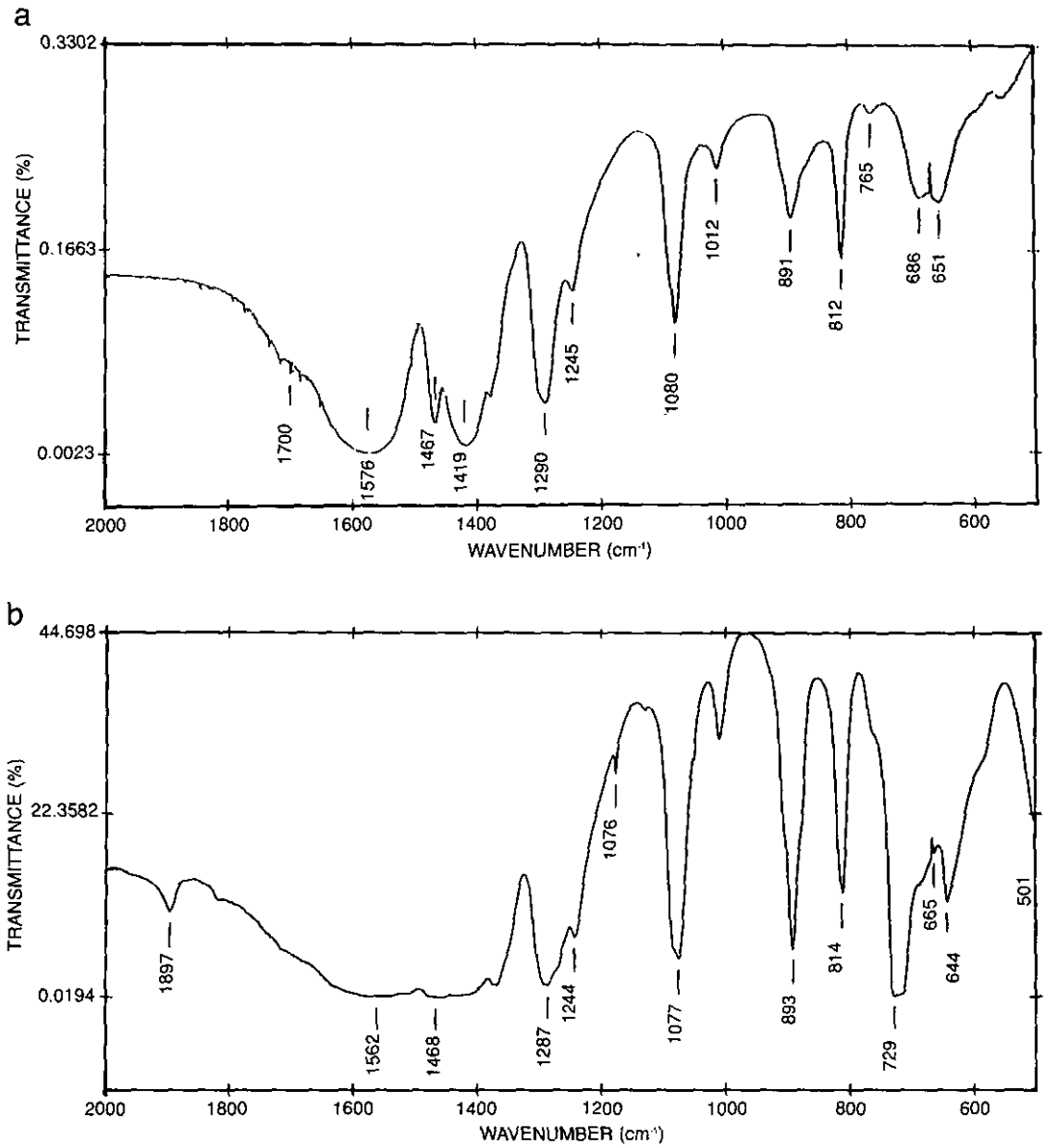

FIG. 3. Transmission IR spectra of the gel precursors on KBr pellets with 1% w/w oxide: (a) Cobalt and nickel propionate gel precursor; heating temperature and time, 180°C and 2 hr. (b) Lanthanum and nickel propionate gel precursor; heating temperature and time, 180°C and 2 hr.

Figure 3a shows the IR spectrum of the gel. One observes bands which correspond to longitudinal metal–oxygen *M*–O vibrations (686, 654 cm^{-1}) besides C–H (1080, 1290, and 1467 cm^{-1}) and C–O (asymmetric and symmetric longitudinal, 1576 and 1419 cm^{-1}) vibrations from the propionic moieties. In addition, bands from CO_3^{2-} (812 cm^{-1}) show that this anion is present, and bands from NO_3^- (894 cm^{-1}) show that even a residual amount of nitrate is still present, despite a series of washings.

Figure 4a shows the continuous TGA–DTA curves of the decomposition of the gel into $NiCo_2O_4$. X-ray diffraction shows that pure $NiCo_2O_4$ was already formed at 350–400°C. The experimental weight loss between room temperature and 400°C is 66%. It can only be said that it is consistent with the proposed formula $NiCo_2(CO_3^{2-})_a(C_3H_5O_2^-)_b(C_3H_6O_2)_c$, assuming $a \ll b + c$, $b \cong 6$ (to compensate the total positive charge on the three metal divalent cations), and $c \cong 1.3$. Neglecting a, one computes 66% from the total combustion reaction by O_2, in close agreement with the experimental value. Calcinations at temperatures/times of 250°C/24 hr, 300°C/1.5 hr, 350°C/3 hr lead equally to the pure spinel phase $NiCo_2O_4$, but calcinations at 450°C/1.5 hr and 600°C/1.5 hr lead to partial decomposition of $NiCo_2O_4$ into NiO and Co_3O_4. The loss of weight above 400°C accounts for such a decomposition, which was also reported by Haenen *et*

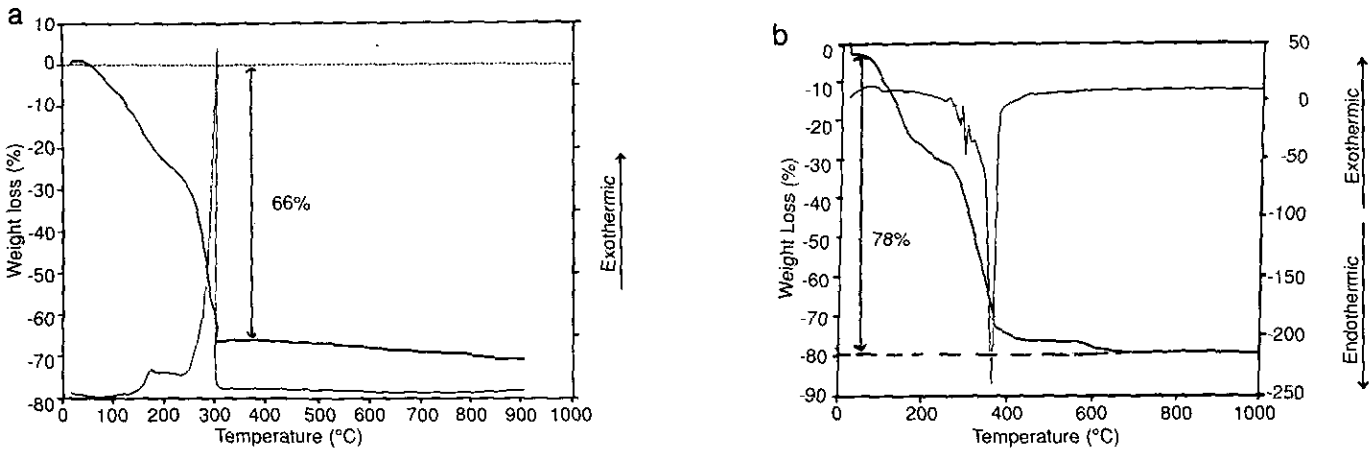

FIG. 4. TGA–DTA curves of pyrolysis in air of the gel precursors. (a) Cobalt and nickel propionate gel precursor; heating rate, 4°C/min. (b) Lanthanum and nickel propionate gel precursor; heating rate, 4°C/min.

al. (19) on $NiCo_2O_4$ freshly prepared by thermal decomposition. At 900°C, Co_3O_4 is likely to be totally decomposed into CoO, on the basis of the numerical analysis of the TGA curve (hypothesizing, however, that at 400°C $NiCo_2O_4$ was perfectly stoichiometric in oxygen). IR transmission spectra are similar to those reported in the literature (20) with metal–oxygen vibration bands of Co(III) (and possibly Ni(III)) in octahedral sites at 559 cm^{-1} (250°C, temperature of preparation) to 568 cm^{-1} (500°C), and of Co(II) in tetrahedral sites at 668–669 cm^{-1} (all temperatures). However, at temperatures of preparations >400°C, the decomposition of $NiCo_2O_4$ was corroborated by the appearance of new bands at 879 and 1437 cm^{-1}, which show the presence of the metal–oxygen bonds of the simple oxides (Co_2O_3, CoO, and NiO). This behavior is different from the behavior of Co_3O_4 prepared by the same sol–gel method (14). In that case, the spinel phase, which was formed around 280–300°C, was perfectly stable at temperatures above 400°C (at least up to 500°C). On the ATD curve one notices a sharp exothermic peak; the reaction was almost explosive, as for Co_3O_4 (14).

Synthesis of $LaNiO_3$ via the Propionic Acid Sol–Gel Type Route

The procedure was identical to the procedure described in the preceding section for $NiCo_2O_4$, but starting with a mixture of lanthanum and nickel carbonates with the ratio La : Ni equal to 1. The TGA curve of pyrolysis of the green gel in air is shown in Fig. 4b. The measured weight loss percentage was 78% between room temperature and 700°C, the temperature at which the pure perovskite phase was formed, as shown by X-ray diffraction. A formula for the gel, similar to the formula proposed in the preceding section for $NiCo_2O_4$, is $LaNi(CO_3^{2-})_a(C_3H_5O_2^-)_b(C_3H_6O_2)_c$. Postulating again $a \ll b + c$, $b \cong 5$ (to compensate the total positive charge on the two metal cations), and $c \cong 7.5$, one accounts for the 78% again neglecting a. The DTA curve indicates that the transformation is endothermic, at variance with the case of the spinels $NiCo_2O_4$ (this work) and Co_3O_4 (Ref. (14)). The transmission IR spectrum of the gel, Fig. 3b, shows bands which correspond to the metal–oxygen M–O vibrations (501, 644, and 665 cm^{-1}). As in Fig. 3a, the bands of CO_3^{2-} (814 cm^{-1}), NO_3^- (893 cm^{-1}), and C–H (1077, 1287, and 1468 cm^{-1}) are present, but the CO bands are not so clear, and a new band at 729 cm^{-1} was not identified.

Synthesis of $LaNiO_3$ via the Malic Acid Route

This synthesis was processed according to Teraoka *et al.* (15). For this, equal mole numbers (35 or 52.5 mM) of $La(NO_3)_3 \cdot 6H_2O$ and $Ni(OH_3)_2 \cdot 6H_2O$ were dissolved in water with 70 or 105 mM of malic acid $C_2H_3OH(COOH)_2$, and the total volume was completed up to 500 or 1000 ml. Different pH's of the solution were fixed with 20% ammonia solution by dropwise addition with constant stirring. pH's higher than 2.5 resulted in precipitation during evaporation, which was not favorable to perovskite phase formation. The resulting solutions were evaporated to dryness to get a viscous transparent gel. This gel was further dried at low temperature to get an almost solid gel. The resulting solid gel was calcined at different temperatures between 550°C and 800°C in presence of air. The gel composition is likely to be $LaNi(NO_3^-)_a(C_4H_4O_5^{2-})_b(C_4H_6O_5)_c(H_2O)_d$, by similarity with the proposed chemical formula for citric acid gels by Anderton and Sale (18). They showed that large numbers of NO_3^- ions were present, as were H_2O molecules. No investigation of the structure and of the pyrolysis mode of the malic gel was made in this work.

The formation of the perovskite phase $LaNiO_3$ was

observed, by X-ray diffraction, at 600°C. With increases of temperature and pH of the initial solution, the X-ray patterns improved. Further, it was observed that initial concentration of the solution plays an important role in the perovskite phase formation.

Nonelectrochemical Characterizations of $NiCo_2O_4$ and $LaNiO_3$ Powders

The characterization techniques for the powders which were used are scanning electron microscopy of spread layers on a solid support, X-ray diffraction, and BET surface area measurements.

(a) $NiCo_2O_4$. Figure 5a shows the X-ray diffractogramm of $NiCo_2O_4$ by the propionic acid method at 350°C. No stray phases are present. The cubic cell parameter was computed $a = 8.119$ Å, which compares well with $a = 8.110$ Å given by the JCPDS ASTM 20-781 file. At temperatures of preparation above 400°C, rays from NiO appear, as expected from the TGA analysis (see above), and the cell parameter tends toward 8.087 Å with increasing temperature, a value close to the cell parameter of Co_3O_4.

The morphology of the powder is shown in Fig. 6a. It can be seen that the layer was finely divided, as expected,

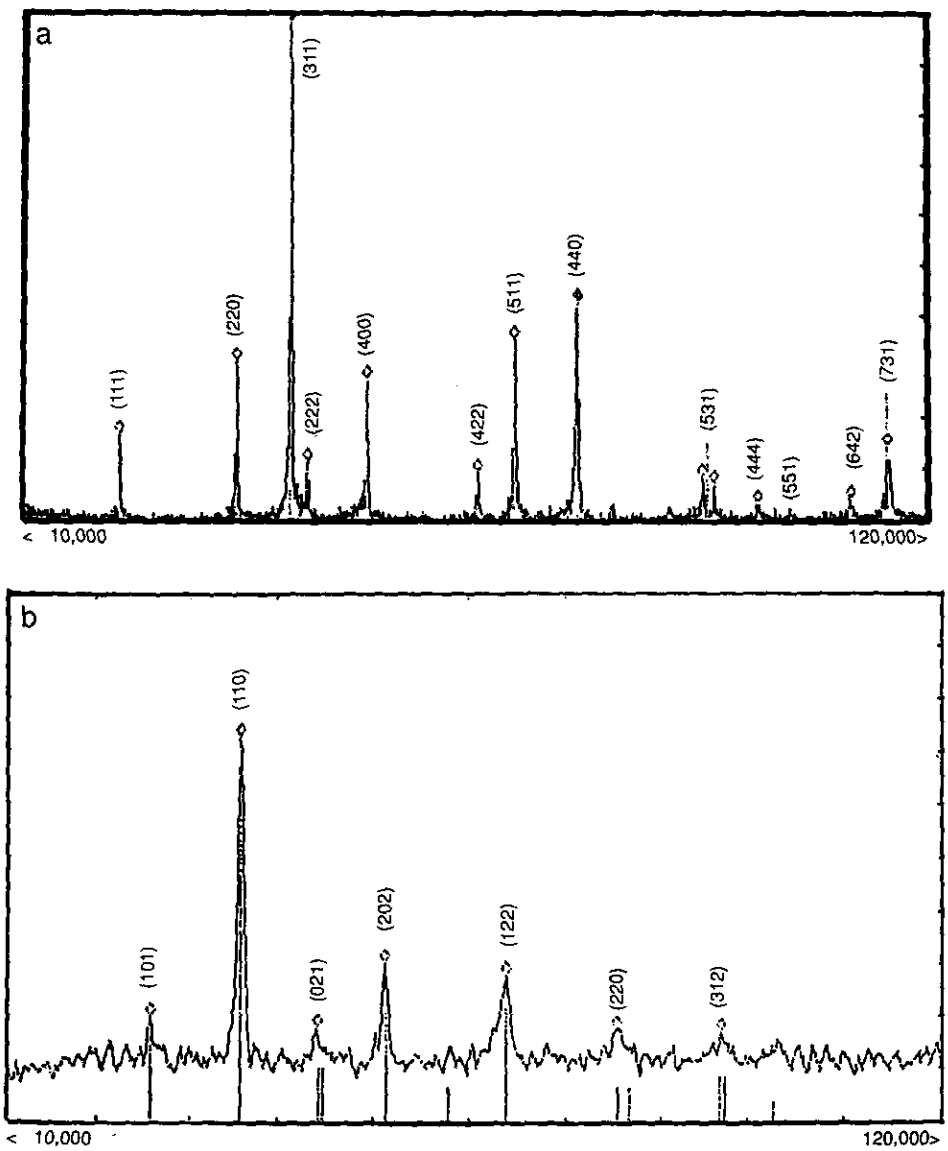

FIG. 5. X-ray diffractograms of the high surface area powders prepared via the propionic acid sol–gel process. (a) $NiCo_2O_4$ (35 $m^2 g^{-1}$); heating temperature and time of the precursor, 350°C and 1.5 hr, in air. (b) $LaNiO_3$ (25 $m^2 g^{-1}$); heating temperature and time of the precursor, 850°C and 6 hr. X-ray diffractograms obtained with $LaNiO_3$ powders prepared (700°C/6 hr) via the malic acid route are similar. Dashed lines show closely spaced rays (003), (024), and (214) near the (021), (220), and (312) rays.

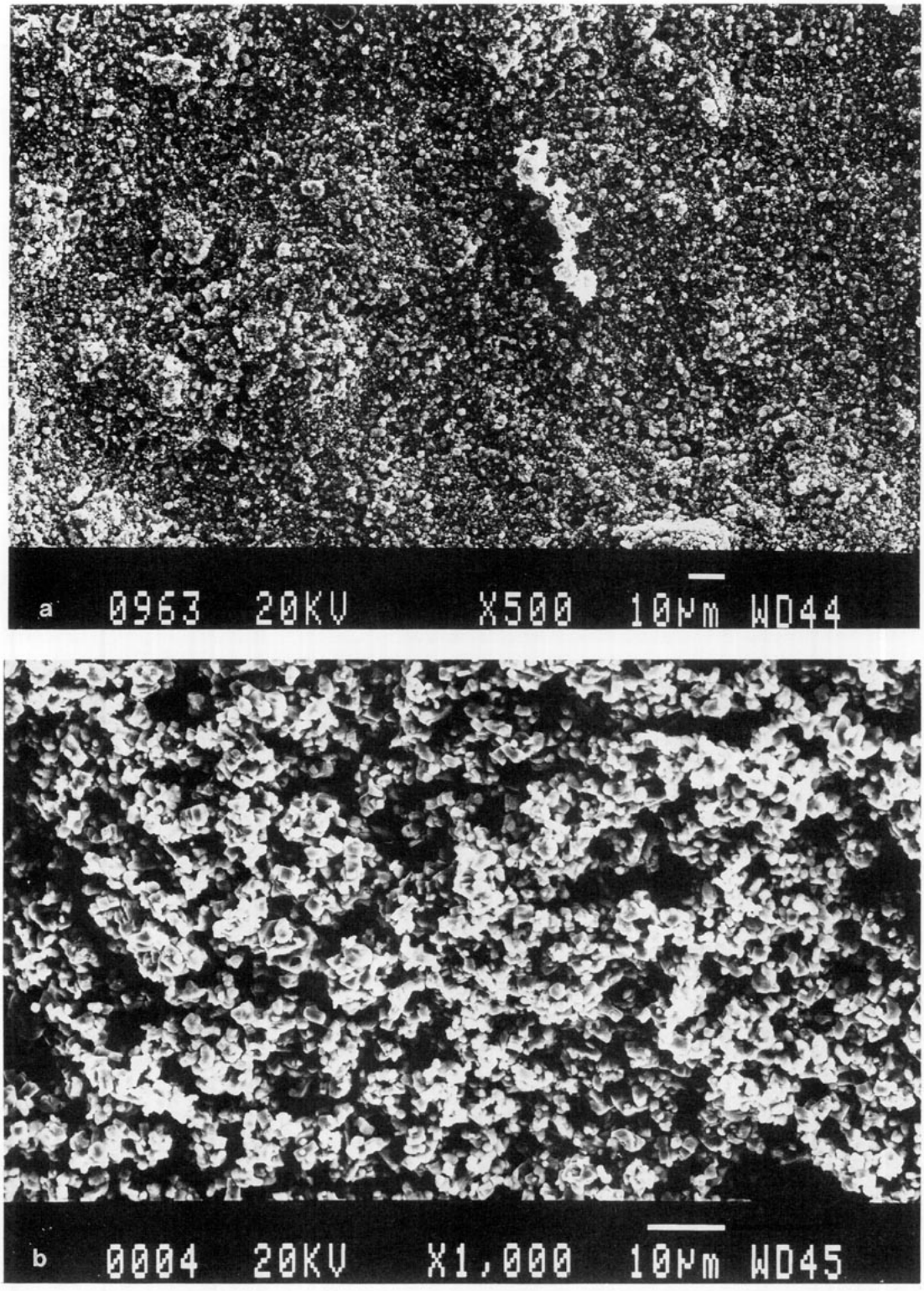

FIG. 6. *Scanning electron microscopy microphotographs of high surface area powders prepared via sol–gel processes and spread on solid substrates by painting:* (a) $NiCo_2O_4$ (46 $m^2\ g^{-1}$) and (b) $LaNiO_3$ (20 $m^2\ g^{-1}$), prepared via the propionic acid sol–gel process; (c) $LaNiO_3$ (8 $m^2\ g^{-1}$) prepared via the malic acid process.

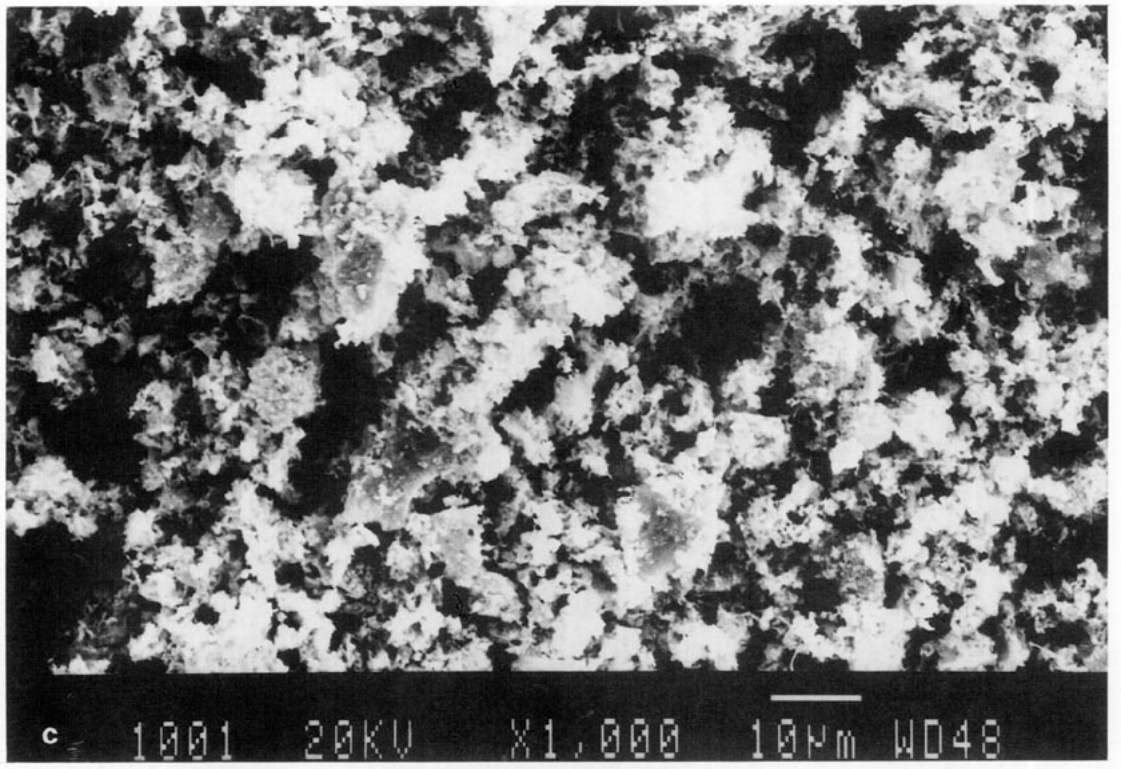

FIG. 6—*Continued*

although it was not made of so regular tiny spheres as was Co_3O_4 prepared by the same method (14).

The BET surface areas are displayed in Table 1a as a function of the temperature and time of preparation and compared to values from the literature (19, 21), for powders obtained by thermal decomposition of the solid-state nitrates. The lower the temperatures and times of preparation, the higher the specific surface area, which can be as high as 53 $m^2 g^{-1}$.

The electrical conductivities were found to be in the order of 0.15 S cm^{-1} (300°C) to 0.35 S cm^{-1} (450°C). Owing to the semiconducting character of $NiCo_2O_4$ (22) the resistance R of a film spread on a quartz plate follows variations, in different temperature ranges, of the type $\ln R = A + B/T$ (A = constant, $B = E_a/R$, with E_a the activation energy in the temperature range and R the molar constant of the perfect gas). Table 2 shows the measured values of E_a (in eV), which compare well with literature values, ranging from 0.06 to 0.4 eV (4, 23, 24). The activation energies differing with the type of gas and with the temperature range reflect changes in the oxygen stoichiometry.

(*b*) *$LaNiO_3$.* Figure 5b shows a typical diffractogram for $LaNiO_3$ prepared either by the propionic acid method or by the malic acid method. In both cases the perovskite was found to crystallize in a hexagonal rhombohedral structure. The unit cell parameters were computed a = 5.465 Å, c = 6.687 Å and a/c = 1.223 (propionic acid method, 850°C/6 hr), a = 5.454 Å, c = 6.578 Å, and a/c = 1.206 (malic acid method, 700°C/6 hr). The JCPDS ASTM file No. 34-1028 gives a = 5.451 Å, c = 6.564 Å, and a/c = 1.204. One sees that the malic acid compound more closely fits the ASTM values than does the propionic acid compound. Note that the malic acid method permits synthesis of $LaNiO_3$ at 650°C, i.e., 100°C below the temperature for propionic acid method. With both methods, crystallinity increases with annealing temperatures, and with the malic acid method with increasing pH and dilution of the initial solution.

The morphologies of the powders shown in Figs 6b and 6c appear to be quite different. $LaNiO_3$ from the propionic acid method shows numerous and well defined monodispersed crystals of ca. 2 µm, whereas $LaNiO_3$ from the malic acid method shows a texture of microcristals which are intimately imbricated.

The Tables 1b and 1c show the specific surface areas as functions of different parameters of preparation (temperature, time, pH). One sees that powders with surface areas as high as 24–25 $m^2 g^{-1}$ were obtained. However, the malic acid method proved to be more advantageous than the propionic acid method, because the pure phase was already obtained at 600°C instead of 750°C.

The energies of activation for conductivity of $LaNiO_3$ prepared by the propionic acid sol–gel method are shown in Table 2. They are on the order of 1 eV, with seemingly two temperature ranges with E_a values differing by ca 20%. They are rather insensitive to the nature of the gas.

TABLE 1

Specific Surface Area of Powders Synthesized via the Different Sol–Gel Methods as a Function of Temperatures and Times of Preparation, via the Propionic Acid Method, for, (a) $NiCo_2O_4$ and (b) $LaNiO_3$, and (c) as a Function of Temperatures of Preparation and pHs, via the Malic Acid Method, for $LaNiO_3$

(a)

Temperature of preparation (°C)	Preparation time (hr)	Specific surface area ($m^2\ g^{-1}$)		
		Propionic acid sol–gel (this work)	Thermal decomposition of nitrates	
			Ref. (19)	Ref. (21)
250	10	54	40	—
300	1	46	32	27
	10	28	16	—
350	1	35	—	18
400	1	24	23	10
	10	15	14	—

(b)

Temperature of preparation (°C)	Preparation time (hr)	Specific surface area ($m^2\ g^{-1}$)
750	6	25
850	6	20
900	6	9
1000	2	4

(c)

Temperature of preparation (°C)	pH		
	1.3[a]	2	2.5
600	[b]	18	24
650	15	17	18
700	11	14	17
800	7	10	11

[a] pH adjusted.
[b] Calcination product was not a single phase.

Surprisingly, we were unable to obtain reproducible ln R vs $1/T$ plots with $LaNiO_3$ from the malic acid method. The resistance of a layer of this compound spread on quartz was found to be about 10^4–10^5 times lower than the resistance of a layer of the propionic acid compound. This shows that thin films of the malic acid product are far more conductive than thin films of the propionic acid compound owing, probably, to the difference in their morphologies.

TABLE 2

Activation Energies for Conductivity of $NiCo_2O_4$ and $LaNiO_3$ Sol–Gel Powders Synthesized via the Propionic Acid Method

	Temperature range (°C)	Activation energies (eV)		
		Argon	Air	Oxygen
$NiCo_2O_4$	60–130	0.13	0.09	0.08
	220–400	0.26	0.20	0.16
$LaNiO_3$	440–560	0.86	0.86	0.93
	636–838	1.03	1.03	1.09

ELECTROCHEMICAL TESTINGS OF SOL–GEL LARGE AREA $NiCo_2O_4$ and $LaNiO_3$ ELECTRODES

The evolution of O_2 from KOH solutions, according to the global reaction

$$4OH^- \rightarrow O_2 + 2H_2O + 4e^-,$$

was chosen as the test reaction. Laboratory test electrodes were of three types: pellets, painted layers on Ni, or painted layers on graphited polyisobutylene foils. Unfortunately, it was not found feasible to realize at will any type of test electrode with any type of pure product, keeping in mind that the objective of the present investiga-

TABLE 3

Feasibility (+) and Unfeasibility (−) of Laboratory Test Electrodes of Pure Sol–Gel Powders of the Investigated Spinel and Perovskite Oxides

Electrodes	Co_3O_4 (propionic acid)	$NiCo_2O_4$ (propionic acid)	$LaNiO_3$ (propionic acid)	$LaNiO_3$ (malic acid)
Pellet	−	−	−	+
Film on Ni foil	+	+	+	−
Film on Poly-isobutylene foil	+	+	−	−

Note. Co_3O_4 from Ref. (14) for comparison.

tion was the testing of the properties of the pure oxides, i.e., oxides unmixed with conductive and binding agents (whereas industrial applications might use such agents). The reason of the unfeasibility of any type of test electrode lies in the particular textures of the sol–gel powders, which are extremely finely divided.

Table 3 shows the test electrodes which were found feasible. Co_3O_4 results from ref [14] were added for completeness. The comparisons of the activities of the different oxides will, therefore, focus on i) Co_3O_4 and $NiCo_2O_4$ (propionic acid) painted on polyisobutylene, ii) $NiCo_2O_4$ (propionic) and $LaNiO_3$ (propionic) painted on Ni foil iii) $LaNiO_3$ (propionic) painted on Ni foil and $LaNiO_3$ (malic) as pellets.

Figures 7a and 7b show typical cyclic voltammograms which were recorded with $NiCo_2O_4$ and $LaNiO_3$ (both propionic). Both reveal the existence of a surface redox couple. For $NiCo_2O_4$, the nature and behavior of the surface redox couple is now well documented in literature. It is ascribed to the redox couple $NiOOH/Ni(OH)_2$ in a thin surface layer (4, 7). In contrast, for $LaNiO_3$ the ascription of the surface redox couple to either a Ni^{IV}/Ni^{III} or Ni^{III}/Ni^{II} redox couple is debated. The double peak is usually poorly visible on pellet materials (25), because it barely emerges from the intense capacitive current which is created by the high electrode surface area (see Fig. 8). We have found that double peaks are particularly well defined only with film electrodes such as in this work (or as in Ref. (10) with sprayed or sequentially coated electrodes).

Co_3O_4 and $NiCo_2O_4$ Sol–Gel (Propionic) Electrodes Painted on Graphited Polyisobutylene

Table 4 shows that the roughness factor of such electrodes (see Experimental) seems to be approximatively proportional to the corresponding powder specific surface area for a given compound, as shown by the two $NiCo_2O_4$ preparations at 400 and 300°C, but that the proportionality ratio depends strongly on the nature of the compound (Co_3O_4 vs $NiCo_2O_4$). The real current density, at 0.7 V vs HgO/Hg, based on the roughness factors, is twice as much on Co_3O_4 as compared to $NiCo_2O_4$, although the *apparent* current density on $NiCo_2O_4$ is equal or higher, being proportional to either the specific areas or the roughness factors. This shows that $NiCo_2O_4$ is intrinsically less active than Co_3O_4, but that large specific surface areas overcompensate for the lesser activity, as expected.

$NiCo_2O_4$ and $LaNiO_3$ Sol–Gel (Propionic) Electrodes Painted on Ni Foils

Table 4 shows that the two powders do have, in fine form, a comparable electroactivity in term of their real current density, but that the apparent current density is

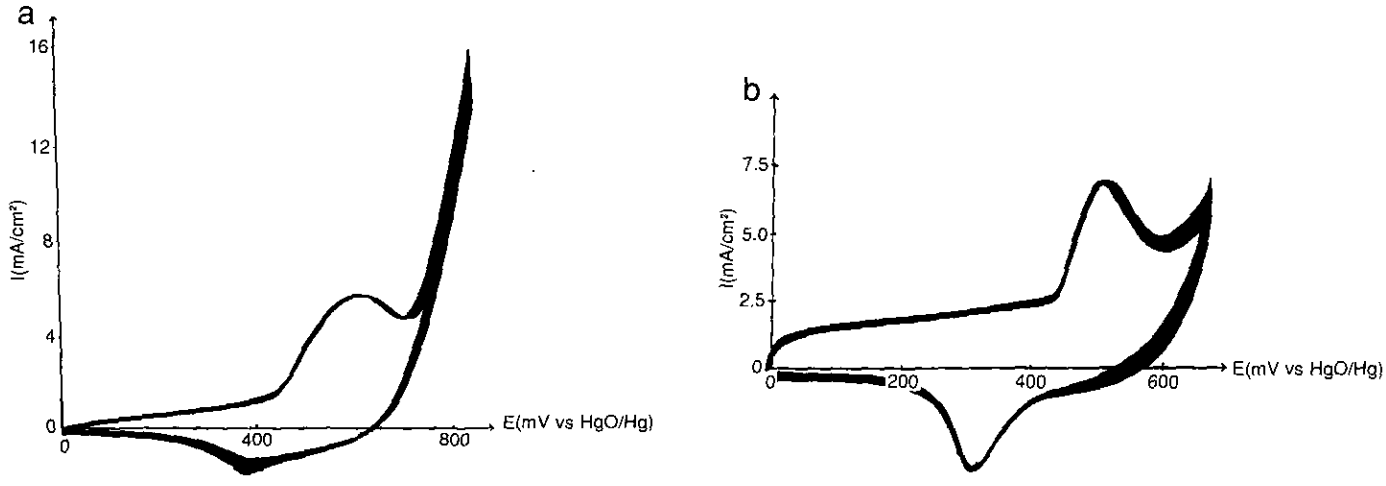

FIG. 7. Stabilized cyclic voltammograms of film electrodes of high surface area catalyst powders painted on nickel. Solution, 1 *M* KOH; temperature, 25°C; scanning rate, 50 mV sec^{-1}. (a) $NiCo_2O_4$ (35 m^2 g^{-1}); number of cycles, 225. (b) $LaNiO_3$ (20 m^2 g^{-1}); number of cycles, 193.

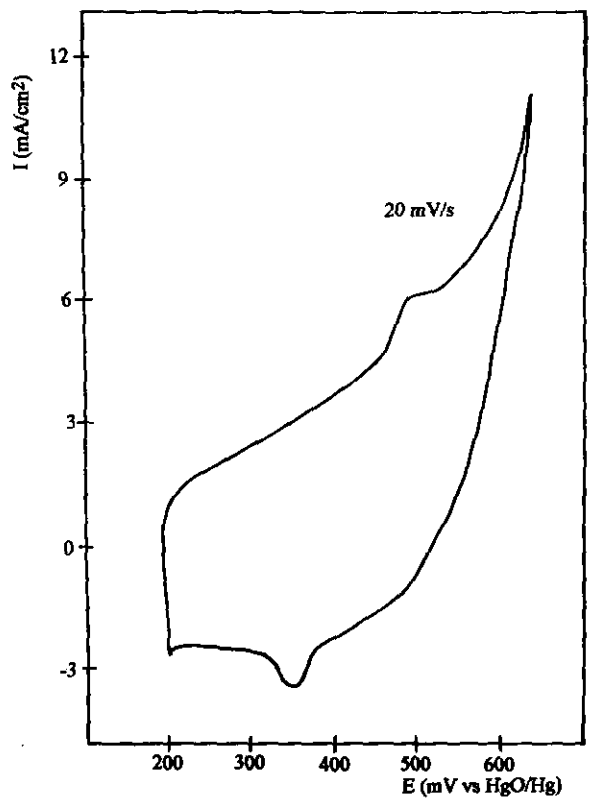

FIG. 8. Cyclic voltammogram of a pellet electrode of the perovskite $LaNiO_3$ prepared via the malic acid sol–gel process (17 $m^2\ g^{-1}$) and made hydrophobic by polystyrene treatment.

about 2–4 times higher with $LaNiO_3$, owing to a 2–4 times larger electrode roughness, depending on the temperature of preparation of $NiCo_2O_4$. Again, one sees that there is no simple relationship between the BET specific surface area and the roughness factor of two different compounds.

$LaNiO_3$ Sol–Gel (Propionic Acid Method) and $LaNiO_3$ Sol–Gel (Malic Acid Method)

The comparison is less straightforward, as the preparation of the test electrodes was different by necessity (Table 3). Continuous evolution of O_2 on pellet electrodes of the pure $LaNiO_3$ (malic acid) powder leads to unstable and continuously decreasing currents under polarization at a fixed potential, due to slow penetration of the electrolyte into the open pores and obstruction by the evolving gas bubbles. Cyclic voltammograms were cycle dependent. To overcome these unstabilities, the pellet electrodes were made hydrophobic with polystyrene (see Experimental). The cyclic voltammograms were then found to be cycle-independent. However, despite the polystyrene treatment, the surface roughness remained high, and the two pseudo-capacity peaks of the surface redox couple still barely emerged from the intense double layer capacity current; see Fig. 8. The estimated roughness factor was as high as ca. 1500, leading to the highest apparent current density of the series but to the smallest real current density.

However, one must be very cautious with this last figure, and consider it as only tentative, because the two test electrodes differ greatly in their preparation mode (film and pellet). It might be that polystyrene, in stabilizing the material, inhibited a fraction of the electroactive centers, thus artificially reducing both apparent and real currents. It is noteworthy, scanning through Table 4, that the roughness factor seems to be proportional to the BET surface area only in the case of the same compound and the same electrode fabrication ($NiCo_2O_4$), but not in cases of different compounds and the same electrode fabrication (Co_3O_4 vs $NiCo_2O_4$), or of the same compound and different electrode fabrications ($LaNiO_3$).

TABLE 4

Main Characteristics of the Sol–Gel Electrodes of Co_3O_4 (from Ref. [14]) and of $NiCo_2O_4$ and $LaNiO_3$ (This Work), Synthesized via the Propionic Acid or Malic Acid Methods

Oxides	Temperature of preparation	σ ($S\ cm^{-1}$)	BET specific surface ($m^2\ g^{-1}$)	Roughness factor ρ	i_{app} ($mA\ cm^{-2}$)	i_{real} ($mA\ cm^{-2}$)
Co_3O_4 (propionic)	300	0.018	28	33	5.0	0.15
$NiCo_2O_4$ (propionic)	400	0.080	24	72	5.6	0.08
$NiCo_2O_4$ (propionic)	300	0.170	46	130	10	0.08
$LaNiO_3$ (propionic)	850	Quasi-metalic	20	270	24	0.09
$LaNiO_3$ (malic)	700	Quasi-metalic	17	1500	27	0.02

Note. The current densities are measured at $E = 0.7$ V vs HgO/Hg on i–V stationary curves; the real current density, i_{real}, is the apparent current, i_{app}, relative to the geometric surface area, divided by the roughness factor, ρ. All electrodes are film electrodes, except malic acid $LaNiO_3$, which is a pellet electrode.

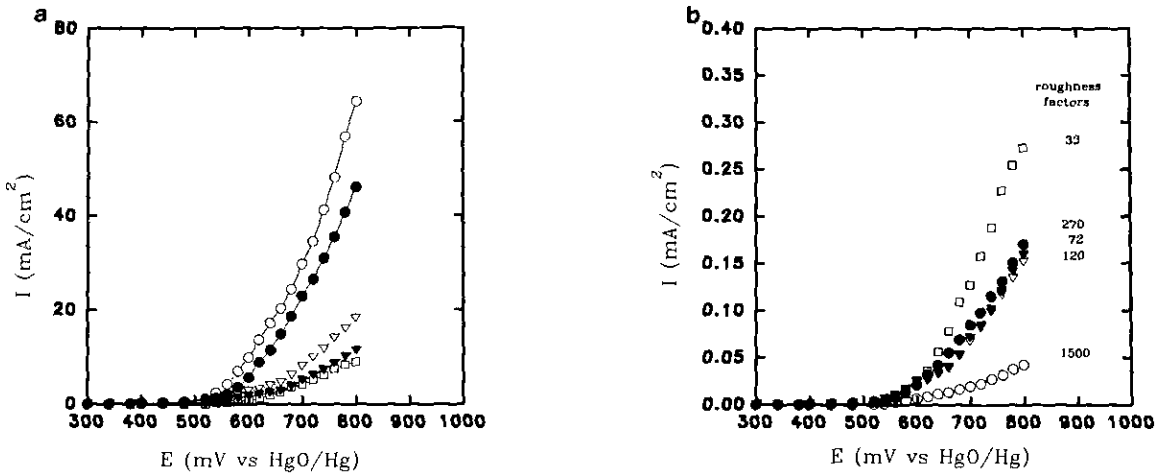

FIG. 9. Rates of evolution of oxygen from aqueous 1 *M* KOH solutions, at 25°C, expressed by the current densities in mA cm^{-2}, on various high surface area sol–gel $LaNiO_3$ and $NiCo_2O_4$ electrodes: (□) Co_3O_4 (350°C) (propionic) and (△) $NiCo_2O_4$ (300°C) (propionic); (▲) $NiCo_2O_4$ (400°C) (propionic), (●) $LaNiO_3$ (propionic), and (○) $LaNiO_3$ (malic). (a) Apparent (experimental) current densities based on geometric areas and (b) real current densities, after correction by roughness factors current, based on real areas.

Figures 9a and 9b show the full apparent (measured) and real (calculated) currents of oxygen evolution on the sol–gel high specific area Ni mixed oxides investigated. Stability testings at room temperature and constant current densities of ca. 25–50 mA cm^{-2} for 50 hr, under continuing O_2 evolution, showed that all test electrodes were quite stable. Industrial applications would require more severe conditions (300–500 mA cm^{-2} at 80°C), which were beyond the scope of this work.

DISCUSSION AND CONCLUSION

This work was undertaken in order to investigate sol–gel process of preparation of oxide electrocatalysts of the oxygen reaction in water. A novel process, using propionic acid, which was recently applied to Co_3O_4 (14) was used. The oxides were the Ni-containing mixed oxides $NiCo_2O_4$ and $LaNiO_3$.

We have confirmed that the propionic acid process yields high specific area powders (20–55 m^2 g^{-1}) at lower temperatures of preparation, especially in the case of $NiCo_2O_4$ (250–300°C), than all non-sol–gel methods. For $LaNiO_3$, however, the hydroxy-acid sol–gel process using malic acid might be more advantageous, because it allows a lower temperature of preparation than the propionic acid process (600 vs 750°C).

The comparative real (intrinsic) electrocatalytical activities were estimated, in each case taking into account the roughness of the electrode. Using film electrodes, the propionic acid method yields $NiCo_2O_4$ and $LaNiO_3$ powders with practically the same real electroactivity (Table 4) and with apparent electroactivity of the same order, differing by only a factor of 2 in favor of the perovskite $LaNiO_3$.

In conclusion, the propionic acid sol–gel process of preparation of finely divided oxides seems to be a very promising method to obtain high surface area electrocatalysts and, presumably catalysts as well.

ACKNOWLEDGMENTS

The authors thank the Centre Franco Indien pour la Recherche Avancée (CEFIPRA, New Delhi) for its support through Project 408-3, for a postdoctoral fellowship in France to S.K.T., and for financial support to M.E.B.

REFERENCES

1. S. Trasatti (Ed.), "Electrodes of Conductive Metallic Oxides," Parts A and B. Elsevier, Amsterdam, 1980.
2. E. J. M. O'Sullivan and E. J. Calvo, *in* "Comprehensive Chemical Kinetics" (R. G. Compton, Ed.), Vol. 27, p. 247. Elsevier, Amsterdam, 1987.
3. L. G. Tejuca, J. L. F. Fierro, and J. M. Tascon, *in* "Advances in Catalysis," Vol. 36. Academic Press, New York, 1989.
4. M. Hamdani, J.-F. Koenig, and P. Chartier, *J. Appl. Electrochem.* **18,** 561 (1988); **18,** 568 (1988).
5. R. N. Singh, M. Hamdani, J.-F. Koenig, J. L. Gautier, G. Poillerat, and P. Chartier, *J. Appl. Electrochem.* **20,** 442 (1990).
6. R. N. Singh, S. K. Tiwari, and P. Chartier, *Indian J. Chem. A* **29,** 837 (1990).
7. R. N. Singh, J.-F. Koenig, G. Poillerat, and P. Chartier, *J. Electrochem. Soc.* **137**(5), 1408 (1990).
8. R. N. Singh, J.-F. Koenig, G. Poillerat, and P. Chartier, *J. Electroanal. Chem.* **314,** 241 (1991).
9. S. K. Tiwari, S. Samuel, R. N. Singh, G. Poillerat, J. F. Koenig, and P. Chartier, *Int. J. Hydrogen Energy,* in press.
10. R. N. Singh, L. Bahadur, J. P. Pandey, S. P. Singh, P. Chartier, and G. Poillerat, *J. Appl. Electrochem.* **24,** 149 (1994).
11. C. H. Marcilly, P. H. Courty, and B. Delmon, *J. Am. Ceram. Soc.* **53,** 56 (1970).
12. P. H. Courty, H. Ajot, C. H. Marcilly, and B. Delmon, *Powder Technol.* **7,** 21 (1973).

13. M. A. Cauqui and J. M. Rodriguez-Izquierdo, *J. Non-Cryst. Solids* **147** & **148,** 724 (1992).
14. M. El Baydi, G. Poillerat, J. L. Rehspringer, J. L. Gautier, J.-F. Koenig, and P. Chartier, *J. Solid State Chem.* **109,** 281 (1994).
15. Y. Teraoka, H. Kakebayashi, I. Moriguchi, and S. Kagawa, *Chem. Lett. (Jpn.)* 673 (1991).
16. E. Calvo, J. Drennan, B. C. H. Steale, and W. J. Albery, *Solid State Ionics*, 294, (1984).
17. S. Levine and A. Smith, *Discussion Faraday Soc.* **52,** 290 (1971).
18. D. J. Anderton and F. R. Sale, *Powder Metall.* **1,** 14 (1979).
19. J. Haenen, W. Visscher, and E. Barendrecht, *J. Electroanal. Chem.* **208,** 298 (1986).
20. J. Preudhomme and P. Tarte, *Spectrochim. Acta* **27,** 1820 (1971).
21. H. M. Carapuca, M. I. Da Silva Pereira, and F. M. A. Da Costa, *Mater. Res Bull.* **25,** 1183 (1990).
22. M. V. Umniskii, V. A. Presnov, A. M. Trunov, O. F. Rakityankaya, T. S. Bakutina, and A. N. Kotseruba, *Elektrokhimiya* **11,** 552 (1975).
23. G. Feuillade, R. Coffe, and G. Outhier, *Ann. Radioelectr.* **21,** 105 (1966).
24. A. M. Trunov, A. A. Domnikov, G. L. Reznikov, and F. R. Yuppets, *Elektrokhimiya* **15,** 783 (1979).
25. E. J. Calvo, J. Drennan, J. A. Kilner, W. J. Albery, and B. C. H. Steele, *Proc. Electrochem. Soc. (Chem. Phys. Electrocatal.)* **84**(12), 489 (1984).